Quantitative determination of the spatial coherence from the visibility of equal-thickness fringes

Kenji Tamasaku* and Tetsuya Ishikawa

RIKEN Harima Institute/SPring-8, Mikazuki, Hyogo 679-5148, Japan. Correspondence e-mail: tamasaku@postman.riken.go.jp

Spatial coherence of the undulator radiation in the horizontal direction is measured by a wedge-shaped crystal interferometer. The Borrmann effect, the effect of the angular divergence of the incidence and the wavefront matching of the collimating asymmetric diffractions with the interferometer are discussed to estimate the coherence factor. The spatial coherence length of 145 µm is experimentally determined, which is enhanced by the collimators about 100 times more than expected from the source size.

1. Introduction

The equal-thickness fringes observed in dynamical X-ray diffraction for incident plane waves (Malgrange & Authier, 1965; Hart & Milne, 1968; Batterman & Hildebrandt, 1968; Kikuta & Kohra, 1968) has been pointed out to be a kind of Young's interferometer by one of the present authors (Ishikawa, 1988). Using bending-magnet radiation of the Photon Factory, the spatial coherence length was estimated semi-quantitatively from the degradation of the visibility of the equal-thickness fringes, like the conventional Young's slits measurements (Born & Wolf, 1975).

Detailed quantification of the coherence of the incident wave requires the effect of finite angular divergence and, in particular, dynamical absorption. The angle-dependent unequal dynamical absorption for two interfering partial waves, well known as the Borrmann effect (Borrmann, 1950), as well as the coherence of the incident beam, degrades the visibility of the equal-thickness fringes.

In this report, a more rigorous treatment is given for the quantitative derivation of both the coherence factor (Born & Wolf, 1975) and the spatial coherence length from the visibility of the equal-thickness fringes by taking dynamical absorption and finite angular divergence into consideration.

2. Principle

The underlying principles are the same as those described in the previous paper (Ishikawa, 1988). Refinement performed in this work includes effects of both finite angular divergence of the incident wave and dynamical absorption in the crystal. Here we consider X-ray diffraction in Laue geometry for a wedge-shaped crystal with an apex angle of β (Fig. 1). For the plane-wave incidence with normalized angular deviation, W, from the exact Bragg condition, the equal-thickness fringe at P is formed by the interference of two partial waves propagating from points A and B on the incident surface along the

Poynting vectors S_1 and S_2. These Poynting vectors are normal to the different branches of the dispersion surface (Kato, 1958; Ewald, 1958). When we choose the X axis perpendicular to the diffracted beam with its origin at the apex of the wedge, the separation, D, between the rays incident at A and B is given by

$$D = \frac{2X|W|\sin\beta\sin\theta_B}{(1+W^2)^{1/2}\cos(\theta_B - \beta)},\tag{1}$$

where θ_B is the Bragg angle.

Since the real incident wave is never an ideal plane wave but with finite angular divergence and spatial extent, we can define the degree of coherence, $|\gamma_{AB}|$, between A and B, as well as the spatial coherence length, σ, for the real incident wave. When D exceeds σ by increasing X, the visibility tends to vanish at the corresponding position, $X = \sigma_X$, which is given by (1) with $D = \sigma$. With the normalized angular divergence, ΔW, of the incident wave, the waves interfering at P come from small regions having width of ΔD around A and B, where

$$\Delta D = \frac{2X\sin\beta\sin\theta_B}{(1+W^2)^{3/2}\cos(\theta_B - \beta)}\Delta W.\tag{2}$$

The finite width of ΔD would further decrease the visibility of the equal-thickness fringe at P from that determined by $|\gamma_{AB}|$. The visibility becomes an integration on the source and the small area around A and B. When both the intensity distribution of the source and the angular intensity distribution of the incidence are Gaussian, the size, s', that decides the visibility is related to the source size, s, and ΔD as

$$(s')^2 = s^2 + (\Delta D)^2.\tag{3}$$

Another factor of decreasing the visibility of the equal-thickness fringes is the unequal absorption for two interfering partial waves in the crystal when dynamical diffraction takes place. The difference in the dynamical linear absorption

coefficient for two branches of the dispersion surface is given by

$$\Delta\mu = \frac{-2|C|K\chi_g''}{(1+W^2)^{1/2}}, \tag{4}$$

where $C = 1$ (σ polarization) or $\cos(2\theta_B)$ (π polarization) is the polarization factor, K is the wave number of X-rays in vacuum and χ_g'' is the imaginary part of the gth Fourier coefficient of the electric polarizability (Pinsker, 1978). The visibility of the equal-thickness fringes for the diffracted wave becomes a function of the thickness, t, and given by

$$V(t) = \frac{I_{\max}(X) - I_{\min}(X)}{I_{\max}(X) + I_{\min}(X)} \tag{5}$$

$$= \frac{|\gamma_{AB}|}{\cosh(\Delta\mu t/2)}, \tag{6}$$

where $t = X\sin\beta/\cos(\theta_B - \beta)$, and $I_{\max}(X)$ and $I_{\min}(X)$ are the upper and lower envelopes of the intensity oscillation of the fringes, respectively. Finite $\Delta\mu$ makes V a monotonic decreasing function of X even if the incident beam is fully coherent, i.e. $|\gamma_{AB}| = 1$, and gives the measurable limit of the equal-thickness fringes, σ_X^{abs}. The degree of the degradation of the visibility caused by $\Delta\mu$ depends on W, so that the W dependence of the pattern of the equal-thickness fringes is needed to confirm (6). Since spatial coherence should be treated by the coherence factor, $|\mu|$, appropriate optics are needed to achieve a condition for $|\mu| \simeq |\gamma_{AB}|$, which will be discussed later.

The measured visibility of the equal-thickness fringes includes both the effect of the dynamical absorption and the true spatial coherence. When the source has a Gaussian intensity distribution, these contributions are written as

$$1/(\sigma_X^{obs})^2 = 1/(\sigma_X)^2 + 1/(\sigma_X^{abs})^2, \tag{7}$$

where σ_X^{obs}, σ_X^{abs} and σ_X are the width of the observed visibility curve, the measurable limit due to the dynamical absorption and the spatial coherence length, which are measured in the X coordinate [equation (1)].
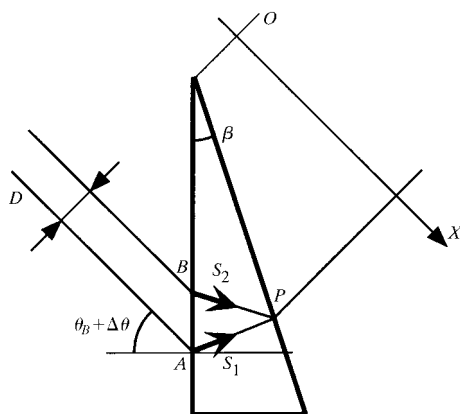
3. Experimental

The experiments were performed at an X-ray undulator beamline, BL29XU, in SPring-8. Water-cooled symmetric Si 111 crystals were used for the double-crystal monochromator. The undulator gap was set to its maximum value, 50 mm, to avoid excess heat load on the first crystal. The radiation was monochromated to be $\lambda_0 = 0.660$ Å, which corresponds to the first harmonic of the undulator at the gap. No thermal broadening was observed in the rocking curve of the first crystal, hence the coherence of the beam was considered to be well preserved. An Si 333 channel-cut crystal was set after the monochromator to make $(+n, +m)$ geometry to reduce the band width of X-rays (Fig. 2). The expected wavelength resolution of the outcoming beam is estimated to be $\Delta\lambda/\lambda_0 = 8.5 \times 10^{-6}$ in the full width at half-maximum (FWHM) from the DuMond analysis (Nakayama et al., 1973). Crystals used in this experiment were prepared from high-quality FZ silicon ingots (Shin-Etsu Semiconductor) with resistivity greater than 1000 Ω cm.

Diffractions after the channel-cut crystal were horizontal, so that the measured visibility of the equal-thickness fringes reflected the horizontal source size. Two successive Si 220 asymmetrically cut crystals collimated the beam. The first one was placed at 53 m from the source and the separation between two asymmetric diffractions is 90 mm. The asymmetric angle, α, and the asymmetric factor, b, at λ_0 were $\alpha = 9.00°$ and $b = 0.0485$ for the first one, and $\alpha = 9.50°$ and $b = 0.0210$ for the second. A wedge-shaped Si 220 crystal with $\beta = 7.59°$ was set in the Laue geometry 250 mm downstream from the second asymmetric diffraction. The angular spread of the collimated beam incident on the wedge-shaped crystal is estimated to be $0.009''$ (FWHM).

First the rocking curve of the wedge-shaped crystal was measured for the diffracted wave. Then the patterns of the equal-thickness fringes were taken from -1.5 to $1.5''$ in steps of $0.25''$ around the Bragg condition. The images were taken by a CCD-based X-ray beam monitor (Hamamatsu Photonics, AA-20MOD) with 25 s integration, spatial resolution of 6 µm and a field of view of 6×6 mm. The stability of the system was

Figure 1
Schematic view of a wedge-shaped crystal interferometer. Two beams incident on points A and B with a separation of D interfere at P.
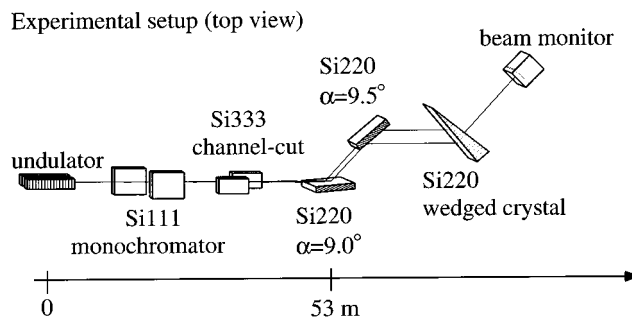

Figure 2
Schematic top view of the experimental set-up. The wavelength resolution is decided by the vertical diffractions at the monochromator and the channel-cut crystal. Two horizontal asymmetric diffractions collimate the beam. The equal-thickness fringes made by the wedge-shaped crystal is observed by a beam monitor.

confirmed by monitoring the beam intensity of the diffracted wave and no drift was observed over 30 min.

4. Results and discussion

Some of the images of the equal-thickness fringes are reproduced in Fig. 3, together with their intensity distributions. The exact deviation angles from the Bragg condition, $\Delta\theta$, were calibrated by the period of the fringes (Ishikawa, 1988), with the *Pendellösung* distance of 42.0 µm and the width of the 220 diffraction of $1.89''$ in π polarization. The angular divergence of $0.009''$ makes the length of ΔD shorter than a few µm for the measured X range [equation (2)], which is much smaller than the horizontal source size. The visibility will be determined by σ and $\Delta\mu$, not by ΔD under the present condition.

To compare the patterns for different Ws, we quantified the width of the visibility curve of the equal-thickness fringes. Shown in Fig. 4 is the visibility curve calculated by equation (5) for $\Delta\theta = -1.55''$. When we fit the visibility by Gaussian as $V(X) = A \exp[-X^2/2(\sigma_X^{obs})^2]$, $\sigma_X^{obs} = 3.76$ mm and $A = 0.93$ would reproduce well the observed curve. We applied the

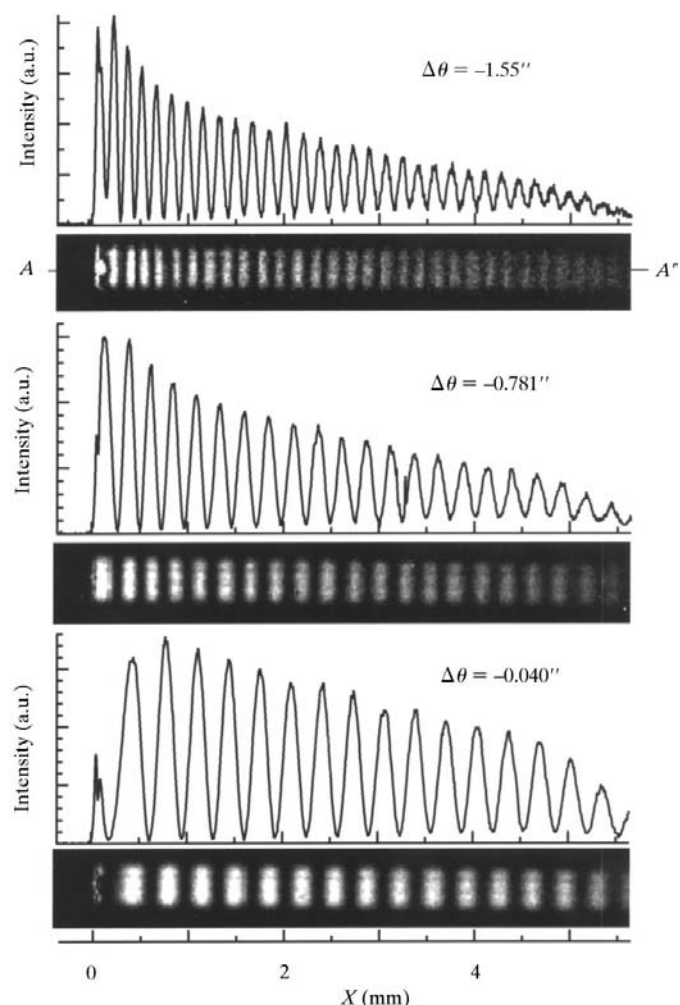same procedure to each image and derived the $\Delta\theta$ dependence of σ_X^{obs} (Fig. 5).

If only the spatial coherence decided σ_X^{obs}, it should have had a $\Delta\theta$ dependence described by (1) with $D = \sigma$, which diverges at $W = 0$. However, σ_X^{obs} seems to be suppressed around $\Delta\theta = 0$ compared with that expected from (1). Such a difference between the measurements and the calculation is accounted for by the dynamical absorption in the wedge-shaped crystal discussed in §2. The measurable limit, σ_X^{abs}, is calculated by (4) and (6) with $\chi_g'' = -1.16 \times 10^{-8}$ under the present condition (Sasaki, 1984). The suppression of σ_X^{obs} around $\Delta\theta = 0$ is well explained by σ_X^{abs}. With (7), the effect of the dynamical absorption was removed and σ_X, which reflects the true spatial coherence length was determined (Fig. 5). Fitting σ_X with (1) gave an estimate of the spatial coherence length of $\sigma = 145$ µm in the standard deviation (STD).

The coherence transfer property of the collimating asymmetric diffractions can be investigated by comparing the horizontal source size with the measured spatial coherence length, $\sigma = 145$ µm. Since the source has a Gaussian intensity distribution with $s = 380$ µm (STD) (Kohmura *et al.*, 2000), the relation between s and σ is represented as

$$\sigma = \lambda L/2\pi s, \tag{8}$$

where L is the distance from the source to the interferometer. The natural spatial coherence length without the collimators is estimated to be 1.5 µm (STD). The spatial coherence length is expanded about 100 times by the two collimating asymmetric diffractions.

Here we would like to emphasize that the wedge-shaped crystal interferometer measures the coherence factor $|\mu(D)|$. When the condition

$$c\tau \ll \lambda_0^2/\Delta\lambda \tag{9}$$

is satisfied, $|\gamma_{AB}(\tau)|$ is nearly equal to $|\mu(D)|$, where $c\tau$ corresponds to the path difference between two beams and c is the light velocity (Born & Wolf, 1975). According to the
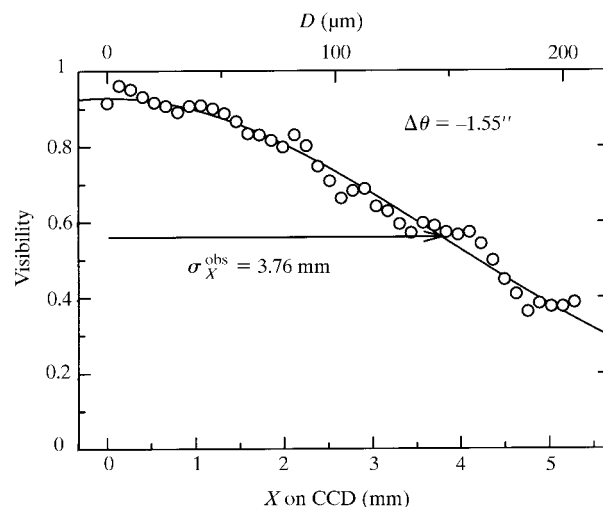

Figure 3
The images of the equal-thickness fringes for some $\Delta\theta$s. The intensity distributions are taken along AA'.

Figure 4
The visibility curve for $\Delta\theta = -1.55''$. The solid line represents a Gaussian fit (see text).

geometrical optics of the asymmetric diffraction (Tamasaku & Ishikawa, 1999), the isochronous wavefront inclines nearly θ_B from the equi-phase wavefront, which is perpendicular to the rays, by a strong collimating asymmetric diffraction ($\alpha \sim \theta_B$). The wavefront inclination angle of 9.89° in the present case is close to the incident angle $\theta_B = 9.90°$. The path difference between points A and B from the source, $c\tau = D \tan(0.01°)$, is negligibly short compared with the estimated temporal coherence length, $\lambda_0^2/\Delta\lambda = 7.8 \, \mu m$ (FWHM), for the measured D range. Thus the wedge-shaped crystal interferometer with highly collimating asymmetric diffractions measures $|\mu(D)|$. When the dynamical absorption does not affect the visibility, e.g. for larger $|\Delta\theta|$ such as $\Delta\theta = -1.55''$, the measured visibility can be regarded as the degree of coherence, i.e. $V(X) \simeq |\mu(D)|$. The intensity distribution of the source is decided by the Fourier transform of $\mu(D)$ using the van Cittert–Zernike theorem. The Gaussian fitting of $V(X)$ is equivalent to the Fourier transformation of $\mu(D)$ because the horizontal intensity distribution of the source is known to be Gaussian.

5. Concluding remarks

We have measured the equal-thickness fringes by a wedge-shaped crystal interferometer and shown that the visibility of the equal-thickness fringes are affected by the dynamical absorption. The effect of the angular divergence on the visibility is much smaller than that of the horizontal source size of the undulator; however, it will be appreciable for the coherence measurement in the vertical direction. After correction for dynamical absorption, we have successfully estimated the coherence factor as well as the spatial coherence length quantitatively. A wedge-shaped crystal interferometer has the ability to measure the coherence factor, $|\mu(D)|$, by a single shot, whereas the conventional Young's slit needs to scan the separation of the double slits, D, for the complete determination of $|\mu(D)|$. One photograph of the equal-thickness fringes is sufficient to determine the size of the source, the intensity distribution of the source and the spatial coherence length.

The wavefront matching between the collimating asymmetric diffractions and the wedge-shaped crystal interferometer, which is enough to measure the coherence factor, is useful for the study of the optics of asymmetric diffraction. The verification of the recent theory on the optics of asymmetric diffraction (Tamasaku & Ishikawa, 1999; Souvorov, 1999) will be presented elsewhere.
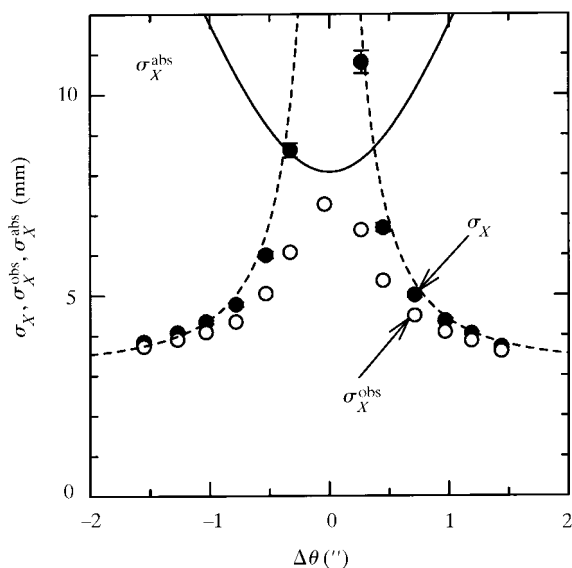
Figure 5
The $\Delta\theta$ dependences of σ_X (closed circles), σ_X^{obs} (open circles) and σ_X^{abs} (solid line). The broken line is a fit to σ_X by equation (1) with $D = \sigma = 145 \, \mu m$.

References

Batterman, B. W. & Hildebrandt, G. (1968). *Acta Cryst.* A**24**, 150–157.
Born, M. & Wolf, E. (1975). *Principles of Optics.* New York: Pergamon.
Borrmann, G. (1950). *Z. Phys.* **127**, 297–323.
Ewald, P. P. (1958). *Acta Cryst.* **11**, 888–891.
Hart, M. & Milne, A. D. (1968). *Phys. Status Solidi*, **26**, 185–189.
Ishikawa, T. (1988). *Acta Cryst.* A**44**, 496–499.
Kato, N. (1958). *Acta Cryst.* **11**, 885–887.
Kikuta, S. & Kohra, K. (1968). *J. Phys. Soc. Jpn*, **25**, 923–924.
Kohmura, Y., Suzuki, Y., Awaji, M., Tanaka, T., Hara, T., Goto, S. & Ishikawa, T. (2000). *Nucl. Instrum. Methods*, A**452**, 343–350.
Malgrange, C. & Authier, A. C. (1965). *C. R. Acad. Sci.* **261**, 3774–3777.
Nakayama, K., Hashizume, H., Miyoshi, A., Kikuta, S. & Kohra, K. (1973). *Z. Naturforsch. Teil A*, **28**, 632–638.
Pinsker, Z. G. (1978). *Dynamical Scattering of X-rays in Crystals.* Berlin: Springer-Verlag.
Sasaki, S. (1984). *Anomalous Scattering Factors for Synchrotron Radiation Users, Calculated Using Cromer and Liberman's Method.* KEK Report 83–22. National Laboratory for High Energy Physics, Japan.
Souvorov, A. (1999). *Proc. SPIE*, **3773**, 14–20.
Tamasaku, K. & Ishikawa, T. (1999). *Proc. SPIE*, **3773**, 207–215.